

Electrochemical Degradation of Synthetic Textile Wastewater by C/MnO₂ Electrode Assessed by Surface Response Methodology



Romuald Tegua Doumbi¹, Guy Bertrand Noumi¹, Domga²

¹Department of Chemistry, Faculty of Science, University of Ngaoundere, PO Box 454, Ngaoundere, Cameroon

²Department of Applied Chemistry, National School of Agro-Industrial Sciences, University of Ngaoundere, PO Box 455 Ngaoundere, Cameroon

*Correspondence to

Romuald Tegua Doumbi,
Tel: +237 695115105,
Fax: (237) 225 17 47,
PO Box 454, Ngaoundere,
Cameroon.
Email: teguiaromuald@yahoo.com,

Published online December 29, 2021



Abstract

The current work investigated the optimization of synthetic textile wastewater (STW) containing methyl orange, crystal violet, and neutral red reactive dye degradation on manganese dioxide coated on graphite electrode using the Box-Behnken design (BBD). Carbon coated by manganese oxide (C/MnO₂) electrode was prepared by the sol-gel method. Graphite substrates were obtained from spent lithium-ion batteries for recycling and reducing the price of the electrode material in electrochemical processes. C/MnO₂ was used as anode and cathode in an electrochemical cell during experiments. In addition, BBD was applied to design the experiments and find the optimal conditions for the degradation of STW. From the proposed model, the rate of the removal efficiency of chemical oxygen demand (COD) reached 83.63% with the optimum conditions (6.989 hours, concentration of 1.5 g/L NaCl, and current density of 50 mA/cm²). Based on the obtained optimum values, the specific energy consumption was around 30.359 kWh (kg COD)⁻¹. Furthermore, the C/MnO₂ electrode was characterized by Raman spectroscopy, and MnO₂ films were prepared from the sol-gel process and deposited on graphite. Thus, using graphite coated with manganese dioxide, indirect anodic oxidation (IAO) can be efficient for the removal of the organic matter from the real textile dye bath.

Keywords: Box-Behnken design, C/MnO₂ electrode, Indirect anodic oxidation, Sol-gel, Synthetic textile wastewater

Received September 7, 2021; Revised November 11, 2021; Accepted December 21, 2021

1. Introduction

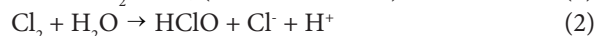
Discharge of textile wastewater into the environment causes higher impacts. Major pollutant charges from textile wastewater are due to several wet-processing operations. The dyeing process uses a huge amount of dyes and produces large amounts of colorful wastewater (1). Approximately 150-350 L of water is required for producing 1 kg of finished apparel. Among the various types of dyes, reactive dyes are widely applied in many cases due to their solubility, durability color, diversity, and low cost (2). These organic pollutants have a complex structure and their degradation is highly challenging. These textile effluents, which are present in the environment, create severe pollution problems by releasing toxic and potentially carcinogenic substances (3). Therefore, their treatment from the environment is an obligation to prevent ecosystem destruction.

Various methods are currently employed for the removal of organic matter from textile wastewater. Although biological, chemical, and physical methods are used for treating dyes (i.e., biological oxidation, incineration, electrocoagulation, adsorption, ozonation, coagulation,

and the like), they cannot sufficiently degrade these effluents (4-6).

In recent years, electrochemical oxidation processes have been suggested as effective and emerging alternatives for the degradation of effluents having high organic matter. Among these methods, electrooxidation has received significant attraction since has easy operation, high energy efficiency, and a fast reaction rate, and is environmentally friendly (7-11). Moreover, the main characteristic of this treatment technic is that it uses electrical energy as a vector for environmental decontamination (12). In these processes, direct or indirect oxidation can be applied to remove pollutants (13). In the indirect anodic oxidation (IAO) process, strong oxidant species such as ozone, hypochlorite/chlorine, or hydrogen peroxide can be generated by electrochemical reactions during electrolysis (14). In the IAO, all the generated oxidants are used during the process. Further, the IAO is more efficient and extensively employed for decontamination due to its simplicity, versatility, and environmental compatibility (15). Furthermore, when chlorine species are generated in the bulk, it is possible to reduce cost-effectiveness and

long residual time and remove microorganisms (16,17). Active chlorine species consisting of dissolved chlorine ($\text{Cl}_{2(\text{aq})}$), hypochlorous acid (HClO), and hypochlorite ion (ClO^-) are electrochemically generated via the chlorine evolution reaction in chloride-containing electrolyte as Eq. (1). In the bulk, hypochlorous acid and hypochlorite ions are obtained after hydrolyzing chlorine (18) and expressed as Eqs. (2) and (3) as follows:



Among the currently used anode in IAO, dimensionally stable anode (DSA), which is made of titanium-based metal covered with a thin conducting of some metal oxides, PbO_2 , SnO_2 -Sb, BDD, and titanium supported platinum (Ti/Pt) electrodes, is extensively applied to oxidize the organic matter from wastewater treatment (19,20). All these materials have a good operating lifetime, good efficiency for the mineralization of pollutants, and high mechanical and electrochemical stability even at high current densities (21). Despite their good electrochemical properties, they are unavailable in developing countries. To fight against their scarcity and high cost, graphite substrate has been chosen in this study to develop electrode materials.

The investigation of cheaper and available electrode materials with analogous performances to DSA and/or BDD has currently attracted great attention in this field (22). The graphite material has been widely employed in electrochemical processes due to its availability and high efficiency for chlorine evolution reactions (23). Among transition metal oxides, MnO_x materials present good electrocatalytic properties, low cost, and low toxicity, and are environmentally friendly. Furthermore, in our previous work, it was shown that the electrochemical properties of graphite (e.g., stability, chlorine evolution potential, and ability to degrade methyl orange [MO]) significantly improved when it recovered from manganese oxide (24).

Some previous studies have focused on evaluating the performance of electrochemical processes in textile wastewater treatment. For instance, Kariyajjanavar et al reported that the maximum removal efficiency of chemical oxygen demand (COD) was 90.5% at a pH rate of 3, NaCl concentration of 25 g/L, current density of 170 Am^{-2} , and electrolysis time of 11 hours (25). In another study, Vatanpour et al showed that the electro-Fenton process is efficient for the treatment of a mixture of two dyes (methyl green and orange II) and found that the maximum color removal efficiency was 98% (26). Ghosh et al also investigated the degradation of synthetic organic dyes by the electro-Fenton process and concluded that high COD removal efficiency for methylene blue was

68%, and the degradation was enhanced by increasing the concentration of hydrogen peroxide (27).

To the best of our knowledge, no study has so far investigated the electrochemical oxidation of three reactive dye bath effluents on manganese oxide electrodes. Thus, the aim of this work was to find the influence of electrolysis factors in the degradation study of synthetic textile wastewater (STW) containing MO, crystal violet (CV), and neutral red (NR) on manganese oxide coated on graphite electrodes. Thus, three factors including electrolysis time, current density, and NaCl concentrations on the degradation efficiency of the synthetic dyeing bath were optimized by the Box-Behnken design (BBD).

2. Materials and Methods

2.1. Chemicals

In this study, graphite is the main material. The samples of graphite were obtained from the used batteries (Tiger Head brand, type R20 UM-1), which were collected and shredded to recover the samples of graphite. These samples had an apparent density of 1.63 g cm^{-3} and an effective area of 12.058 cm^2 . Silver sulfate, mercuric sulfate, sodium chloride, sodium sulfate, sodium thiosulfate, MO, CV, and NR were of analytical grade and were purchased from Merck Company (Germany). Isopropanol and manganese chloride ($\text{MnCl}_2 \cdot 4\text{H}_2\text{O}$), as well as sodium hydroxide and sulfuric acid were purchased from Prolabo (Swiss) and Sigma-Aldrich (USA) Companies, respectively.

2.2. Electrocatalyst Preparation

The C/ MnO_2 electrode was prepared by a simple sol-gel method according to our previous work (24). Typically, the substrates must be deprived of grease and stripe to ensure a uniform thickness of the deposited layer. Substrates were washed using acetone. Then, they were sandblasted in alumina for five minutes, treated by the chemical treatment in oxalic solution 10% for 45 minutes, and dried at 105°C for 5 minutes (28). Next, the substrate was ready to receive coating MnO_2 films.

To prepare the solution of manganese dioxide, a mixture of isopropanol and manganese chloride was heated at 80°C in processing reflux for 45 minutes. Then, a permanganate solution was quickly added to the mixture. Afterward, 5 mL of acetic acid was added to the medium after 2 hours. The process took 4 hours. This synthesis-based method was reported by Chen et al (29) with some modifications.

After the pretreatment of substrates, they were recovered by the MnO_2 using the dip-coating technique. Materials were dried at 105°C for 15 minutes and burned at 400°C for 5 minutes in the furnace for the deposition of one layer. The previous steps were repeated occasionally. After the deposition of the latest layer, the materials were burned at 400°C for 2 hours. These temperatures are selected with the aim to obtain the most stable manganese

dioxide. This is inspired by the works of Cardarelli et al (28) and Lin et al (30).

2.3. Electrode Characterization

Raman analysis is highly suited for molecular morphology characterization of carbon materials. Each vibrational frequency of a bond within the molecule corresponds to a band. The laser Raman microscope (LabRAM HR, Horiba, Italia) equipped with diode laser operating at 633 nm wavelength was employed to collect Raman spectra.

2.4. The Electrochemical Process

Synthetic wastewater was prepared by dissolving 0.3 g MO, 0.3 g CV, 0.3 g NR, 0.1 g Na_2SO_4 , 0.1 mg. Na_2CO_3 , 0.1 g of NaOH, and 0.1 g K_3PO_4 in 1 L of distilled water, which are the main components in real textile industry wastewater (31,32). Then, the synthetic effluent was hydrolyzed by heating at 50°C for 1 hour (11). The synthetic wastewater was electrochemically oxidized in a bath reactor (150 mL) equipped with two electrodes of C/ MnO_2 as anode and cathode in conjunction with an adjustable power supply unit (LW LONG WEI LK-K30100, China, Fig. 1). The distance between the electrodes was fixed at 1 cm. The duration of all the electrolysis experiments was varying. A magnetic stirrer (Mivaris Magnetic Stirrer, England) was used to mix the solution. For all experiments, the pH of the solution was fixed at 3 because some studies have been realized to optimize the pH during the IAO of reactive dyes, and their results demonstrated that a low pH level leads to the high oxidation of the organic matter. However, at a low acidic medium, Cl_2 and HClO are the main oxidizing species present during electrolysis, which have higher oxidation potential compared to ClO^- (6,24).

2.5. Analytical Methods

In this study, the COD removal efficiency was used to evaluate the rate of organic matter degradation. The COD (mgO_2/L) of the solution was determined during electrolysis by the closed reflux titrimetric method with

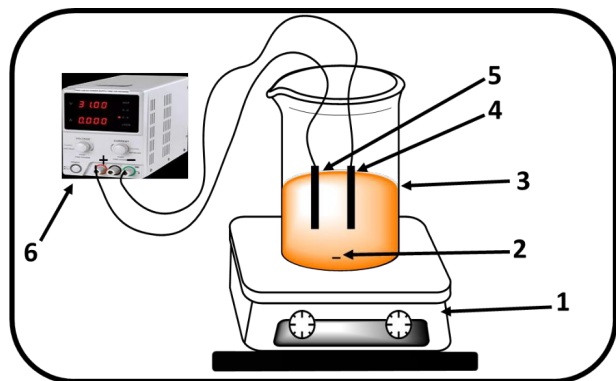


Fig. 1. The Experimental Set-up: (1) Magnetic stirrer, (2) Magnetic bar, (3) Electrolytic cell, (4) Cathode (C/ MnO_2), (5) Anode (C/ MnO_2), and (6) D.C Power Supply. Note. MnO_2 : Carbon coated by manganese oxide.

the titrant of ammonium ferrous sulfate hexahydrate. The method is based on the oxidation of the organic matter by dichromate in the acidic solution in the heater apparatus (Hachi, USA) at 150°C for 2 hours (33). The COD removal efficiency was computed according to Eq. (4):

$$\text{COD removal (\%)} = \frac{(\text{COD}_0 - \text{COD}_t)}{\text{COD}_0} \times 100 \quad (4)$$

where COD_0 and COD_t are the solution COD values at the initial and t time of the electrolysis, respectively.

Ammonium, nitrate, nitrite, sulfate, carbonate, and phosphate ions were determined according to the methods described by Rodier et al (33). The characteristics of the STW are summarized in Table 1.

2.6. Experimental Design

Response surface methodology (RSM) is based on the exploration of the relationships between several explanatory variables and one or more response variables. The main idea of RSM is to use a sequence of designed experiments to obtain optimum operating conditions. In this study, three factors including current density, electrolysis time, and NaCl concentration were chosen to design a matrix of an experiment using the BBD. Each factor was studied at three levels coded as -1 (low), 0 (medium), and +1 (high) for a total of 16 experiments.

The second-order polynomial quadratic model for predicting the optimum value of three factors can be stated according to Eq. (5):

$$Y = \beta_0 + \sum \beta_1 X_1 + \sum \beta_2 X_2 + \sum \beta_3 X_3 + \sum \beta_{12} X_1 X_2 + \sum \beta_{13} X_1 X_3 + \sum \beta_{23} X_2 X_3 + \sum \beta_{11} X_1^2 + \sum \beta_{22} X_2^2 + \sum \beta_{33} X_3^2 \quad (5)$$

where Y and β_0 indicate predicted responses and offset term (Intercept process effect), respectively. In addition, β_1 , β_2 , and β_3 are linear effects. Likewise, β_{11} , β_{22} , and β_{33} denote squared effects. Further, β_{12} , β_{13} , and β_{23} are cross-product effects. Moreover, $X_1 X_2$, $X_1 X_3$, and $X_2 X_3$ represent the interactions. This model demonstrates the quadratic effect of X_1 , X_2 , and X_3 . The RSM was used to determine the optimum experimental conditions for maximum degradation. This methodology is a collection of statistical tools for showing the effect of some variables influencing the responses by varying them simultaneously (34). The results of the optimization study were analyzed using STATGRAPHIC Centurion XVI software.

3. Results and Discussion

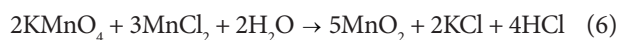
3.1. Electrocatalyst Characterizations

The manganese dioxide colloidal suspension was prepared by the sol-gel process. The pH of this solution was 1.85, revealing the formation of the hydrochloric acid during the process according to Eq. (6).

Table 1. Characteristics of the Synthetic Dye Bath

Characteristics	Unit	Value Before Treatment	Value After Treatment
pH (20°C)	-	10.3 ± 0.1	10.9 ± 0.1
Conductivity	µS/cm	5610 ± 50	2150 ± 30
Temperature	°C	20 ± 1	22 ± 1
COD	mgO ₂ /L	721 ± 11	118.03 ± 2.14
[SO ₄ ²⁻]	mg/L	98.12 ± 1.55	14.23 ± 1.89
[CO ₃ ²⁻]	mg/L	99.25 ± 0.64	47.25 ± 1.66
[PO ₄ ³⁻]	mg/L	97.36 ± 1.76	73.1 ± 3.56

Note. COD: Chemical oxygen demand.



Visible spectra (Fig. 2a) were measured to study the optical property of the MnO₂ sol. This spectrum presents a maximum absorption in the visible area at 390 nm. Generally, the absorption spectrum of MnO₂ solution is 350.2-403.4 nm. Mulvaney et al (35) obtained a wavelength at 360 nm, which proves the presence of MnO₂ particles in the obtained solution.

Raman spectroscopy is widely applied for the characterization of MnO₂ doped carbon composites given its sensitivity to both MnO₂ oxidation state and carbon structural properties (36). The Raman spectra of graphite and manganese oxide coated on graphite substrates are shown in Fig. 2b. First, the Raman spectrum of graphite presents three peaks, which are denominated D (1348 cm⁻¹), G (1575 cm⁻¹), and 2D (2668 cm⁻¹) bands. The crystalline structure of graphite is attributed to the G band, which is the main peak and is also associated with the symmetric E_{2g} vibrational mode in the graphite structure and to the sp² bonded carbon atoms in a two-dimensional hexagonal lattice. The disorder and defect in the graphitic structure are related by the D band. The latter peak is the 2D band, which is also attributed to the sp²-bonded carbon atoms in a two-dimensional lattice and connotes that the graphite sheet contains some layers (37). In the spectrum of manganese oxide coated on graphite, the same peaks are observed that are present in

the Raman spectrum of graphite materials. However, it is important to specify that the observed bands are wider compared to the graphitic bands, except for the 2D band which is low. These observations imply that the sample of graphite has been oxidized, proving the presence of the Mn-O group on its surface. The birnessite-type MnO₂ peak is observed at around 642 cm⁻¹ (34,38). The intensity ratio of D and G bands (I_D/I_G) is used to determine the degree of disorder and defect in graphitic materials. The intensity ratios (I_D/I_G) of the graphite and the manganese oxide coated on graphite were 0.1 and 1.09, respectively. However, it is noteworthy that the highest intensity ratio belongs to the as-prepared material. This growth can be explained by the effect of the electrostatic interaction between manganese oxide with the carbon in the form of graphite and the increasing amount of defects (39). Thus, MnO₂ onto graphite was successfully synthesized based on the results of Raman spectra.

3.2. Optimization of Electrochemical Degradation of the Organic Matter on C/MnO₂

3.2.1. Data Analysis

The organic matter degradation was evaluated by the COD removal efficiency. Current density (X_1), electrolysis time (X_2), and NaCl concentration (X_3) were the main variables. The experimental and predicted results are presented in Table 2.

Exp and pre are the experimental and predicted values of COD removal efficiency.

In this study, the rate of COD removal varied between 58.256% and 82.2548%. The mathematical model, Eq. (5), which gives the interaction between independent factors and COD removal efficiency is expressed by Eq. (7).

$$Y = 34.7977 + 0.834897 X_1 + 5.55774 X_2 - 0.52488 X_3 - 0.000989206 X_1^2 - 0.0520675 X_1 X_2 - 0.164182 X_1 X_3 - 0.0823375 X_2^2 + 0.421458 X_2 X_3 + 0.7187 X_3^2 \quad (7)$$

where Y represents the predicted COD removal efficiency, and X_1 , X_2 , and X_3 are current density, time,

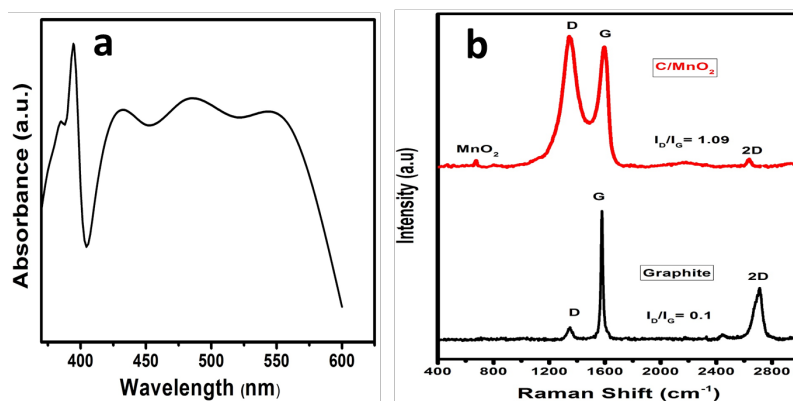


Figure 2. (a) Visible Spectrum of the MnO₂ Solution and (b) Raman Spectra of Graphite and MnO₂ Coated Onto Graphite. Note. MnO₂: Carbon coated by manganese oxide.

Table 2. Full Factorial Design Used for the IAO of STW on the C/MnO₂ Electrode

Run N°	X ₁ : j(mA/cm ²)	X ₂ : t(h)	X ₃ : [NaCl](g/L)	COD Removal Efficiency (%)	
				Y _{exp} (%)	Y _{pre} (%)
1	50	5	2.5	76.152	74.708
2	50	5	1.5	78.3256	78.4599
3	30	5	2.0	73.35	73.0631
4	30	5	2.0	72.95	73.0631
5	10	5	2.5	70.6523	70.518
6	30	7	2.5	79.4552	81.1313
7	30	5	2.0	72.9513	73.0631
8	30	5	2.0	73.0013	73.0631
9	30	7	1.5	80.6589	80.7566
10	50	7	2.0	82.2548	82.0227
11	30	3	2.5	64.3251	64.2274
12	30	3	1.5	67.2146	65.5385
13	10	7	2.0	80.2562	78.7145
14	50	3	2.0	68.5854	70.1271
15	10	3	2.0	58.256	58.4881
16	10	5	1.5	66.2586	67.7026

Note. IAO: Indirect anodic oxidation; STW: Synthetic textile wastewater; COD: Chemical oxygen demand; MnO₂: Carbon coated by manganese oxide.

and [NaCl], respectively. As shown, current density and operating time have a positive effect on the response, while NaCl concentration has a negative effect. Furthermore, electrolysis time (X₂) has the highest effect on the response.

The ANOVA test was used to analyze experimental data in order to validate the model (Table 3). Current density, electrolysis time, and NaCl concentration, as well as the quadratic effect between current density and electrolysis time, between current density and NaCl concentration, and between electrolysis time and NaCl concentration have a low *P* value (*P*<0.05). Based on *P* value and *F*-test results (Table 3), the quadratic model for *Y* was highly significant, and the *F*-value was 17.767 for the functions corresponding to *Y*. Furthermore, the R² coefficient was 0.977971, which is high and shows that 97.797% of the observed variability in data can be explained by the predicted model. The adjusted R² square (R²_{adj}=0.944953) is also high. Based on these values, the predicted model

was highly significant. The lack of a fit test for the final model was insignificant (*P*=0.153), confirming the fit of this model. Furthermore, the Anderson-Darling test for normality was insignificant, approving this assumption of the model.

Pareto analysis was employed to further interpret the results according to (Eq. 8) as follows (4):

$$P_i = \frac{b_i^2}{\sum b_i^2} \times 100 \quad (i \neq 0) \quad (8)$$

where *b* is the related regression coefficient of the parameter. Fig. 3 displays the Pareto graphic analysis and the influence of each independent factor and their interaction on the COD removal efficiency. As shown, electrolysis time and current density have a positive effect and are the most determining factors on COD removal efficiency. [NaCl], the interaction between electrolysis time and current density and the interaction between [NaCl] and current density exert a negative effect and are the most determining factors on the COD removal efficiency. The negative effect of these factors implies that they have an antagonist impact on COD removal efficiency. Moreover, the other interactions have a negligible effect on the response.

3.2.2. Influence of the Electrolysis Parameter on COD Removal Efficiency

The model Eq. (8) was used in this part to develop the response surface and contour plots. These graphs lead to a further understanding of the effect of each factor and their interaction on COD removal efficiency. Fig. 4 shows the effect of the interaction between current density and time on COD removal efficiency. Based on the data, COD removal efficiency increases with current density and time. Isik et al (40) studied the degradation of textile dyeing bath by electrooxidation using activated carbon cloth as electrodes and found that the maximum COD removal was 95.5% at the current density of 100 A/m² for 90 minutes. In this work, the optimum value of the COD removal was 83.63% at the current density of 50 mA/cm² for 6.9 hours. The difference can be ascribed to the high usage of current density and the presence of 4254 mg/L of the NaCl concentration that are important factors during electrooxidation. More current density provides high generation of oxidizing species which promote high the

Table 3. Statistical Indices Obtained From the ANOVA for COD Removal Efficiency

Source	Sum of Squares	Degrees of Freedom	Mean Square	F Value	P Value	R ² Values
Model	658.0952	6	109.6825	17.767	< 0.0001	R ² =97.797
Residuals	4.059576	9	0.45106			R ² _{adj} =94.4953
Lack of fit	12.5716	8	1.57145			
Pure error	1.6161	1	1.6161			
Total	676.3424	15	113.3211			

Note. ANOVA: Analysis of variance; COD: Chemical oxygen demand.

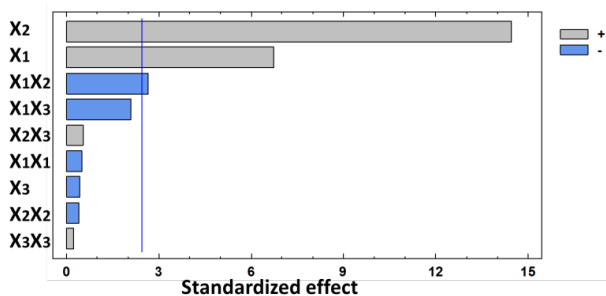


Fig. 3. Pareto Graphic Analysis.

oxidation of the organic matter and high COD removal.

The interaction between current density and [NaCl] on the response at a constant electrolysis time of 5 hours is depicted in Fig. 5. According to these graphs, at low [NaCl], COD removal efficiency increases with current density. In other words, increasing current density leads to the generation of a large quantity of active chlorine species that rapidly react with organic pollutants, leading to greater degradation of the organic matter (6,41). Furthermore, higher current densities contribute to a reduction in the efficiency of the process generating low hypochlorite, which converts to a chloro-oxidant of higher oxidation states and is expressed as Eq. (9). Thus, it is important to notice that the oxidation of STW has a limit current where the efficiency is the highest.



The obtained data in Fig. 6 indicate that an increase in [NaCl] leads to a decrease in response, while increasing the reaction time enhances the degradation of the organic matter. Hence, it is noteworthy that excessive Cl^- ion concentrations seem to have a negative effect on the treatment of STW using IAO. During the process, the degradation is mainly attributed to the chlorine species (Cl_2 , HClO , and ClO^-) which are electrogenerated in the bulk according to Eqs. (1), (2), and (3). In our previous work investigating the degradation of MO on C/MnO_2 , the optimum value of COD removal was 77.0% (24). In this work, an optimal value of 83.629% of COD removal was obtained for STW containing MO, CV, and NR. The observed difference may be because the inorganic salts present in the bulk play an important role during the electrochemical oxidation process. However, the OH^- radical may oxidize inorganic ions to yield strong oxidants such as perphosphate, percarbonate, and persulfate, as expressed by Eqs. (10), (11), and (12), which can indirectly oxidize organic pollutants (42,43). More precisely, they contribute to the production of some oxidants in the bulk which react with the organic matter and destroy it. Eqs. (10)-(13) represent the reactions that could be formed in the bulk giving the oxidizing species.

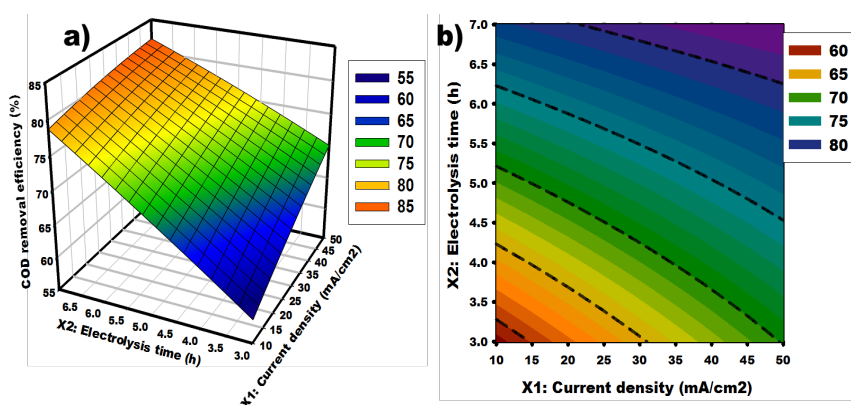


Fig. 4. Response Surface and Contour Graphs for COD Removal From Synthetic Textile Wastewater: Effect of Current Density and Time. Note. Chemical oxygen demand.

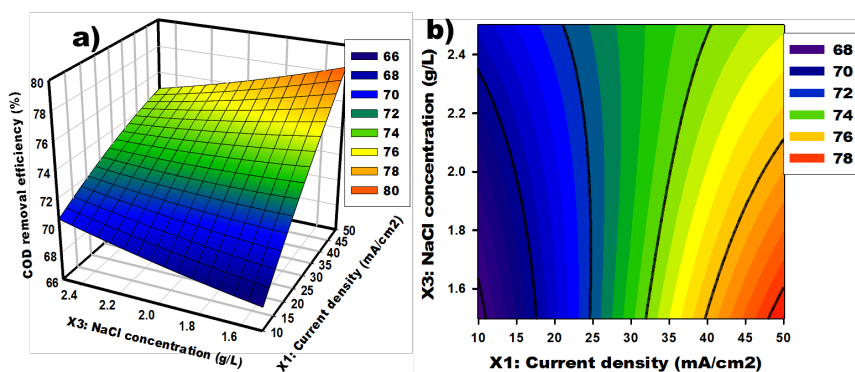


Fig. 5. Response Surface and Contour Graphs for COD Removal From Synthetic Textile Wastewater: Effect of Current Density and NaCl Concentration. Note. Chemical oxygen demand.

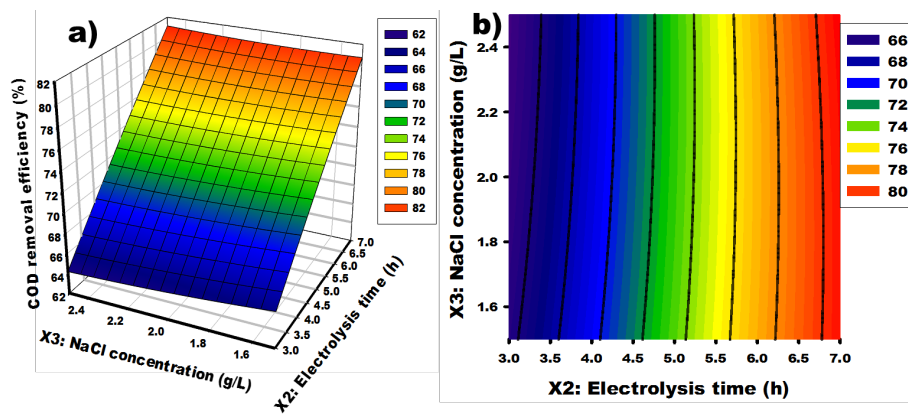


Fig. 6. Response Surface and Contour Graphs for COD Removal From Synthetic Textile Wastewater: Effect of Electrolysis Time and NaCl Concentration. Note. Chemical oxygen demand.



Moreover, hydroxyl radicals could be generated at the surface of the manganese oxide electrode. $\cdot\text{OH}$ radicals have high oxidation potential and quickly react with organic pollutants (R) according to Eqs. (14) and (15) as follows (15,44):



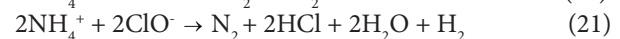
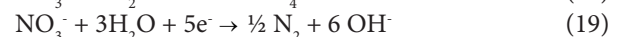
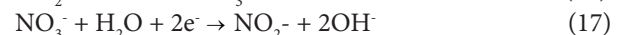
3.2.3. Determination of Optimal Removal Conditions and Model Validation

The optimum values of the independent variables are presented in Table 4. Under the obtained optimum conditions, the maximum COD removal efficiency was 83.63%. From these optimum conditions, three experiments were performed, and the average COD removal efficiency was 81.521%, which is in agreement with the predicted value of 83.63% for 6.9 hours of electrolysis.

3.3. Evolution of Inorganic Ions

From the optimum conditions obtained based on the optimization results, our work focused on determining each inorganic ion during the electrolysis of STW (Fig. 7). Our findings showed that during the operation time, the degradation of reactive dyes automatically generates

inorganic ions such as nitrate, nitrite, and ammonium. These compounds are toxic and represent a high risk for aquatic systems and human health when they are discharged into the environment without treatment. During the process, nitrate and nitrite were slightly generated, while ammonium ions were highly generated before 4 hours of electrolysis, and then its concentration demonstrated a decrease. The slow generation of nitrite ions can be explained by the fact that during the operation time, NO_2^- ions are oxidized to NO_3^- in the presence of HClO according to Eq. (16). Furthermore, NO_3^- can be reduced on the cathode into nitrite, ammonium, and nitrogen according to Eqs. (17), (18), and (19), respectively (45). This is why the NH_4^+ is highly generated. The reduction of nitrate at the cathode generates NO_2^- , which is oxidized to NO_3^- according to the reaction expressed by Eq. (16), leading to a decrease in the nitrate concentration in the bulk. After 4 hours of electrolysis, the NH_4^+ concentration decreased in the bulk. This is probably due to the indirect oxidation of ammonium into nitrogen gas by the hypochlorous and hypochlorite ions generated during the electrolysis, as shown in the reactions in Eqs. (20), and (21) as follows (46,47):



During the experiment, the concentrations of SO_4^{2-} , CO_3^{2-} , and PO_4^{3-} decreased in the function of time. The decreasing of sulfate and carbonate ions was more significant than that of the PO_4^{3-} which seems to be constant. Indeed, this is probably because SO_4^{2-} and CO_3^{2-} are converted into persulfate and percarbonate ions during the process, respectively. This experiment justifies the fact that high COD removal is obtained in this study

Table 4. Optimum Operational Conditions of the Indirect Anodic Oxidation of Synthetic Textile Wastewater

Variables	Value	COD Removal Efficiency (%)
X_1 : Current density (mA/cm ²)	50.0	
X_2 : Electrolysis time (hours)	6.989	83.63
X_3 : NaCl concentration (g/L)	1.50	

Note. COD: Chemical oxygen demand.

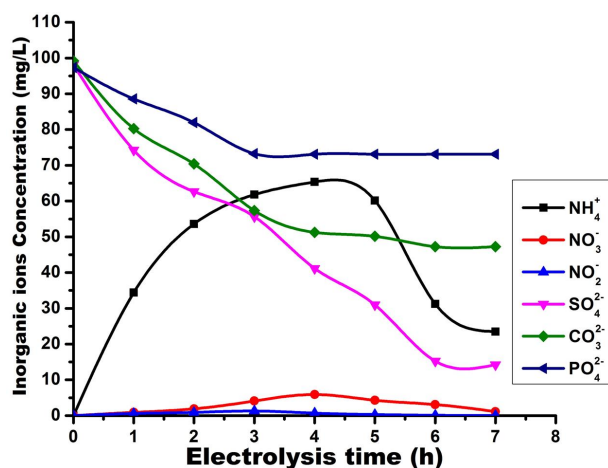


Fig. 7. Evolution of the Concentration of Inorganic Ions Versus Time During the Electrolysis, Current Density (50 mA/cm²), and NaCl Concentration (1.5 g/L).

because persulfate and percarbonate further oxidize the reactive dyes and promote their degradation.

3.4. Specific Energy Consumption

Eq. (22) is usually used to evaluate the energy consumption during electrochemical oxidation processes. It is expressed per g of removed COD (48).

$$Esp = \frac{I \times U \times t}{[(COD)_0 - (COD)_t] \times V} \quad (22)$$

where (COD)₀ and (COD)_t are the COD value of STW and the treated STW, mgO₂/L, respectively. I is the current intensity. In addition, A: U and V: t are the potential and the reaction times, respectively. Further, h and V are the volumes of STW and L. According to the optimum value of COD removal efficiency, the energy consumption was 30.359 (kWh)/kg COD in this work. Sánchez-Sánchez et al (12) found that the specific energy consumption was around 21.87 kWh/kg COD (lower than the recent study) during the treatment of textile effluents by electrochemical oxidation. Ghosh et al also evaluated the specific energy consumption for the treatment of the synthetic dye bath containing methylene blue dye and obtained a maximum COD removal of 80% and specific energy of 20.85 kWh/kg COD (27). The observed difference in the results could be due to the large COD concentration in this work and distinct electrode characteristics. The optimum operating region was found to be applicable for the electrochemical degradation of the organic matter from STW.

4. Conclusion

In the current work, the electrochemical oxidation of STW using the C/MnO₂ electrode was assessed by RSM. Used batteries were employed as a substrate for the development of C/MnO₂ electrocatalyst by the sol-gel route. Characterization results based on Raman spectroscopy proved the deposition of MnO₂ particles on the graphite surface. The BBD demonstrated that the

most influent factors are current density and electrolysis time for COD removal efficiency. Thus, IAO with NaCl leads to the almost complete removal of COD from STW. More precisely, 83.63% of COD removal was obtained under certain conditions (6.989 hours of electrolysis, 1.5 g/L of NaCl concentration, and 50 mA/cm² of current density). The results also revealed that during electrolysis, reactive dyes are degraded to inorganic ions (NO₃⁻, NO₂⁻, and NH₄⁺) which can be oxidized or reduced to nitrogen at the end of the process when the electrolysis takes a long time. IAO using the modified graphite material as the electrode is an efficient method for textile wastewater treatment and can be applied for other textile wastewaters.

Acknowledgements

The authors of this work would like to address their sincere gratitude to the Department of Chemistry of the Faculty of Science at the University of Ngaoundere for making all the necessary resources available for this work. The authors also want to thank Mr. NYAMSI Max for his technical help with this research.

Conflict of Interest Disclosures

The authors have no conflict of interests.

Ethical Statement

All procedures of this work were in agreement with the ethical standards of the institutional and/or national research committee.

References

1. Mcheik AH, El Jamal MM. Kinetic study of the discoloration of rhodamine B with persulfate, iron activation. *J Chem Technol Metall.* 2013;48(4):357-65.
2. Bonyadinejad G, Sarafraz M, Khosravi M, Ebrahimi A, Taghavi-Shahri SM, Nateghi R, et al. Electrochemical degradation of the Acid Orange 10 dye on a Ti/PbO₂ anode assessed by response surface methodology. *Korean J Chem Eng.* 2016;33(1):189-96. doi: 10.1007/s11814-015-0115-x.
3. Marković M, Jović M, Stanković D, Mutić J, Roglić G, Manojlović D. Toxicity screening after electrochemical degradation of reactive textile dyes. *Pol J Environ Stud.* 2014;23(6):2103-9. doi: 10.15244/pjoes/28298.
4. Rahmani Z, Samadi MT. Preparation of magnetic multi-walled carbon nanotubes to adsorb sodium dodecyl sulfate (SDS). *Avicenna J Environ Health Eng.* 2017;4(1):61902. doi: 10.5812/ajehe.61902.
5. Domga R, Harouna M, Tcheka C, Tchatchueng JB, Tsafam A, Domga KN, et al. Batch equilibrium, kinetic and thermodynamic studies on adsorption of methylene blue in aqueous solution onto activated carbon prepared from *Bos indicus* gudali bones. *Chem J.* 2015;1(6):172-81.
6. Oukili K, Loukili M. Optimization of textile azo dye degradation by electrochemical oxidation using Box-Behnken design. *Mediterr J Chem.* 2019;8(5):410-9. doi: 10.13171/mjc851907103ko.
7. Santos JEL, de Moura DC, da Silva DR, Panizza M, Martínez-Huitle CA. Application of TiO₂-nanotubes/PbO₂ as an anode for the electrochemical elimination of Acid Red 1 dye. *J Solid State Electrochem.* 2019;23(2):351-60. doi: 10.1007/s10008-018-4134-5.
8. Panizza M, Cerisola G. Electrochemical degradation of methyl red using BDD and PbO₂ anodes. *Ind Eng Chem Res.* 2008;47(18):6816-20. doi: 10.1021/ie8001292.
9. Syam Babu D, Anantha Singh TS, Nidheesh PV, Suresh Kumar

- M. Industrial wastewater treatment by electrocoagulation process. *Sep Sci Technol.* 2020;55(17):3195-227. doi: [10.1080/01496395.2019.1671866](https://doi.org/10.1080/01496395.2019.1671866).
10. Nidheesh PV, Zhou M, Oturan MA. An overview on the removal of synthetic dyes from water by electrochemical advanced oxidation processes. *Chemosphere.* 2018;197:210-27. doi: [10.1016/j.chemosphere.2017.12.195](https://doi.org/10.1016/j.chemosphere.2017.12.195).
 11. Patabandige DS, Wadumethrige SH, Wanniarachchi S. Decolorization and COD removal from synthetic and real textile dye bath wastewater containing Reactive Black 5. *Desalin Water Treat.* 2020;197:392-401. doi: [10.5004/dwt.2020.25954](https://doi.org/10.5004/dwt.2020.25954).
 12. Sánchez-Sánchez A, Tejocote-Pérez M, Fuentes-Rivas RM, Linares-Hernández I, Martínez-Miranda V, Fonseca-Montes de Oca RMG. Treatment of a textile effluent by electrochemical oxidation and coupled system electrooxidation–*Salix babylonica*. *Int J Photoenergy.* 2018;2018:3147923. doi: [10.1155/2018/3147923](https://doi.org/10.1155/2018/3147923).
 13. Mazaheri Tehrani A, Dehghani R, Soheil Arezoomand HR, Gilaasi HR, Tavakoli Z. Degradation of formaldehyde from synthetic wastewater using Fe²⁺/H₂O₂/O₃ process. *Avicenna J Environ Health Eng.* 2017;4(2):1-5. doi: [10.15171/ajehe.2017.01](https://doi.org/10.15171/ajehe.2017.01).
 14. Afanga H, Zazou H, Titchou FE, Rakhila Y, Akbour RA, Elmchaouri A, et al. Integrated electrochemical processes for textile industry wastewater treatment: system performances and sludge settling characteristics. *Sustain Environ Res.* 2020;30(1):2. doi: [10.1186/s42834-019-0043-2](https://doi.org/10.1186/s42834-019-0043-2).
 15. Teguia DR, Noumi GB, Akoulah JL, Domga. Indirect electrochemical degradation of methyl orange dye on graphite bifunctional electrode. *Int J Appl Res.* 2020;6(1):1-13. doi: [10.6084/m9.figshare.12161202](https://doi.org/10.6084/m9.figshare.12161202).
 16. Ha H, Jin K, Park S, Lee KG, Cho KH, Seo H, et al. Highly selective active chlorine generation electrocatalyzed by Co₃O₄ nanoparticles: mechanistic investigation through in situ electrokinetic and spectroscopic analyses. *J Phys Chem Lett.* 2019;10(6):1226-33. doi: [10.1021/acs.jpcclett.9b00547](https://doi.org/10.1021/acs.jpcclett.9b00547).
 17. Stupar SL, Grgur BN, Onjia AE, Mijin D. Direct and indirect electrochemical degradation of acid blue 111 using IrOx anode. *Int J Electrochem Sci.* 2017;12(9):8564-77. doi: [10.20964/2017.09.44](https://doi.org/10.20964/2017.09.44).
 18. Britto-Costa PH, Ruotolo LA. Phenol removal from wastewaters by electrochemical oxidation using boron doped diamond (BDD) and Ti/TiO₂.7RuO₃O₂ dsa® electrodes. *Braz J Chem Eng.* 2012;29(4):763-73. doi: [10.1590/s0104-66322012000400008](https://doi.org/10.1590/s0104-66322012000400008).
 19. Peralta-Hernández JM, Méndez-Tovar M, Guerra-Sánchez R, Martínez-Huitle CA, Nava JL. A brief review on environmental application of boron doped diamond electrodes as a new way for electrochemical incineration of synthetic dyes. *Int J Electrochem.* 2012;2012:154316. doi: [10.1155/2012/154316](https://doi.org/10.1155/2012/154316).
 20. Salazar R, Ureta-Zañartu MS, González-Vargas C, do Nascimento Brito C, Martínez-Huitle CA. Electrochemical degradation of industrial textile dye disperse yellow 3: Role of electrocatalytic material and experimental conditions on the catalytic production of oxidants and oxidation pathway. *Chemosphere.* 2018;198:21-9. doi: [10.1016/j.chemosphere.2017.12.092](https://doi.org/10.1016/j.chemosphere.2017.12.092).
 21. Maamar M, Bellakhal N. Treatment of a Tunisian textile effluent containing bromothymol blue dye using anodic oxidation on boron doped diamond electrode. *J Tunisian Chem Soc.* 2017;19:32-42.
 22. Nair KM, Kumaravel V, Pillai SC. Carbonaceous cathode materials for electro-Fenton technology: mechanism, kinetics, recent advances, opportunities and challenges. *Chemosphere.* 2021;269:129325. doi: [10.1016/j.chemosphere.2020.129325](https://doi.org/10.1016/j.chemosphere.2020.129325).
 23. Domga, Domga R, Noumi GB, Tchatchueng JB. Study of some electrolysis parameters for chlorine and hydrogen production using a new membrane electrolyzer. *Int J Chem Eng Anal Sci.* 2017;2(1):1-8.
 24. Teguia Doumbi R, Noumi GB, Domga. Dip coating deposition of manganese oxide nanoparticles on graphite by sol gel technique for the indirect electrochemical oxidation of methyl orange dye: parameter's optimization using Box-Behnken design. *Case Stud Chem Environ Eng.* 2021;3:100068. doi: [10.1016/j.csee.2020.100068](https://doi.org/10.1016/j.csee.2020.100068).
 25. Kariyajanavar P, Narayana J, Nayaka YA. Degradation of textile wastewater by electrochemical method. *Hydrol Current Res.* 2011;2(1):110. doi: [10.4172/2157-7587.1000110](https://doi.org/10.4172/2157-7587.1000110).
 26. Vatanpour V, Daneshvar N, Rasoulifard MH. Electro-Fenton degradation of synthetic dye mixture: influence of intermediates. *J Environ Eng Manage.* 2009;19(5):277-82.
 27. Ghosh P, Thakur LK, Samanta AN, Ray S. Electro-Fenton treatment of synthetic organic dyes: influence of operational parameters and kinetic study. *Korean J Chem Eng.* 2012;29(9):1203-10. doi: [10.1007/s11814-012-0011-6](https://doi.org/10.1007/s11814-012-0011-6).
 28. Cardarelli F, Taxil P, Savall A. Tantalum protective thin coating techniques for the chemical process industry: molten salts electrocoating as a new alternative. *Int J Refract Metals Hard Mater.* 1996;14(5-6):365-81. doi: [10.1016/S0263-4368\(96\)00034-0](https://doi.org/10.1016/S0263-4368(96)00034-0).
 29. Chen S, Zhu J, Han Q, Zheng Z, Yang Y, Wang X. Shape-controlled synthesis of one-dimensional MnO₂ via a facile quick-precipitation procedure and its electrochemical properties. *Cryst Growth Des.* 2009;9(10):4356-61. doi: [10.1021/cg900223f](https://doi.org/10.1021/cg900223f).
 30. Lin CK, Chuang KH, Lin CY, Tsay CY, Chen CY. Manganese oxide films prepared by sol-gel process for supercapacitor application. *Surf Coat Technol.* 2007;202(4-7):1272-6. doi: [10.1016/j.surfcoat.2007.07.049](https://doi.org/10.1016/j.surfcoat.2007.07.049).
 31. Körbahti BK, Turan KM. Evaluation of energy consumption in electrochemical oxidation of acid violet 7 textile dye using Pt/Ir electrodes. *J Turk Chem Soc A Chem.* 2016;3(3):75-92. doi: [10.18596/jotcsa.31804](https://doi.org/10.18596/jotcsa.31804).
 32. Ponce de León C, Vasconcelos VM, Rosiwal S, Lanza MR. Electrochemical degradation of Reactive Blue 19 dye by combining boron doped diamond and reticulated vitreous carbon electrodes. *ChemElectroChem.* 2019;6(13):3516-24. doi: [10.1002/celec.201900563](https://doi.org/10.1002/celec.201900563).
 33. Rodier J, Bernard L, Nicole M. L'analyse physico-chimique et microbiologique de l'eau-9ème édition, Paris-Dunod. (2009). 2556-3521.
 34. Kayan B, Akay S, Kulaksız E, Gözmen B, Kalderis D. Acid Red 1 and Acid Red 114 decolorization in H₂O₂-modified subcritical water: process optimization and application on a textile wastewater. *Desalin Water Treat.* 2017;59:248-61. doi: [10.5004/dwt.2017.0552](https://doi.org/10.5004/dwt.2017.0552).
 35. Mulvaney P, Cooper R, Grieser F, Meisel D. Charge trapping in the reductive dissolution of colloidal suspensions of iron(III) oxides. *Langmuir.* 1988;4(5):1206-11. doi: [10.1021/la00083a028](https://doi.org/10.1021/la00083a028).
 36. Najafpoor AA, Davoudi M, Rahmanpour Salmani E. Decolorization of synthetic textile wastewater using electrochemical cell divided by cellulosic separator. *J Environ Health Sci Eng.* 2017;15:11. doi: [10.1186/s40201-017-0273-3](https://doi.org/10.1186/s40201-017-0273-3).
 37. Domga T, Noumi GB, Sieliechi MJ, Tchatchueng JB. Synthesis of nitrogen and phosphorus co-doped graphene as efficient electrocatalyst for oxygen reduction reaction under strong alkaline media in advanced chlor-alkali cell. *Carbon Trends.* 2021;4:100043. doi: [10.1016/j.cartre.2021.100043](https://doi.org/10.1016/j.cartre.2021.100043).

38. Park CS, Zhao Y, Shon Y, Yoon CS, Lee H, Lee CJ. Observation of ferromagnetic semiconductor behavior in manganese-oxide doped graphene. *AIP Adv.* 2014;4(8):087120. doi: [10.1063/1.4893240](https://doi.org/10.1063/1.4893240).
39. Muzyka R, Drewniak S, Pustelny T, Chrubasik M, Gryglewicz G. Characterization of graphite oxide and reduced graphene oxide obtained from different graphite precursors and oxidized by different methods using Raman spectroscopy. *Materials (Basel)*. 2018;11(7):1050. doi: [10.3390/ma11071050](https://doi.org/10.3390/ma11071050).
40. Isik Z, Ozbey Unal B, Karagunduz A, Keskinler B, Dizge N. Electrochemical treatment of textile dye bath wastewater using activated carbon cloth electrodes. *Avicenna J Environ Health Eng.* 2020;7(1):47-52. doi: [10.34172/ajehe.2020.07](https://doi.org/10.34172/ajehe.2020.07).
41. Valica M, Hostin S. Electrochemical treatment of water contaminated with methylorange. *Nova Biotechnol Chim.* 2016;15(1):55-64. doi: [10.1515/nbec-2016-0006](https://doi.org/10.1515/nbec-2016-0006).
42. Panizza M, Cerisola G. Direct and mediated anodic oxidation of organic pollutants. *Chem Rev.* 2009;109(12):6541-69. doi: [10.1021/cr9001319](https://doi.org/10.1021/cr9001319).
43. Radjenovic J, Sedlak DL. Challenges and opportunities for electrochemical processes as next-generation technologies for the treatment of contaminated water. *Environ Sci Technol.* 2015;49(19):11292-302. doi: [10.1021/acs.est.5b02414](https://doi.org/10.1021/acs.est.5b02414).
44. Tahir H, Shah AR, Iqbal S, Kifayatullah HM. The statistical optimization of indirect electrochemical oxidation process for the treatment of dye from simulated textile discharge. *Int J Environ Sci Nat Resour.* 2017;2(2):555583. doi: [10.19080/ijesnr.2017.02.555583](https://doi.org/10.19080/ijesnr.2017.02.555583).
45. Xu D, Li Y, Yin L, Ji Y, Niu J, Yu Y. Electrochemical removal of nitrate in industrial wastewater. *Front Environ Sci Eng.* 2018;12(1):9. doi: [10.1007/s11783-018-1033-z](https://doi.org/10.1007/s11783-018-1033-z).
46. Ghimire U, Jang M, Jung SP, Park D, Park SJ, Yu H, et al. Electrochemical removal of ammonium nitrogen and COD of domestic wastewater using platinum coated titanium as an anode electrode. *Energies.* 2019;12(5):883. doi: [10.3390/en12050883](https://doi.org/10.3390/en12050883).
47. Cifcioglu-Gozuacik B, Ergenekon SM, Ozbey-Unal B, Balcik C, Karagunduz A, Dizge N, et al. Efficient removal of ammoniacal nitrogen from textile printing wastewater by electro-oxidation considering the effects of NaCl and NaOCl addition. *Water Sci Technol.* 2021;84(3):752-62. doi: [10.2166/wst.2021.261](https://doi.org/10.2166/wst.2021.261).
48. Zhang G, Huang X, Ma J, Wu F, Zhou T. Ti/RuO₂-IrO₂-SnO₂ anode for electrochemical degradation of pollutants in pharmaceutical wastewater: optimization and degradation performances. *Sustainability.* 2021;13(1):126. doi: [10.3390/su13010126](https://doi.org/10.3390/su13010126).